In situ UV-VIS diffuse reflectance spectroscopy of reduction–reoxidation of heteropoly compounds by methanol and ethanol: a correlation between spectroscopic and catalytic data

J. Melsheimer [a,*], Sabri S. Mahmoud [b], G. Mestl [a] and R. Schlögl [a]

[a] *Fritz-Haber-Institut, Max Planck Gesellschaft, Faradayweg 4-6, D-14195 Berlin, Germany*
[b] *Chemistry Department, Yarmouk University, Irbid, Jordan*

Received 22 December 1998; accepted 27 April 1999

The degree of reduction/oxidation of $H_4PVMo_{11}O_{40}$ (HPA) and $Cs_2H_2PVMo_{11}O_{40}$ (CsPA) was studied during reduction and reoxidation by methanol, ethanol and mixtures with oxygen, respectively. The peak intensity of the intervalence charge transfer (IVCT) band, the apparent band gap energy (E_g^*) and catalytic data were obtained by *in situ* UV-VIS diffuse reflectance spectrosccopy (UV-VIS-DRS) and on-line gas chromatography (GC), respectively. The peak intensity of the IVCT band and E_g^* increase during the reduction of heteropoly compounds by the alcohols. The spectroscopic and catalytic data (conversion, selectivity) correlate in the transient state during the reoxidation process. It is shown that isolated Keggin anions act as precursors for the active states of the catalysts, which molecular structure cannot be deduced from UV-VIS spectroscopy alone. UV-VIS spectroscopy, however, can serve as a tool to determine the degree of reduction in future combined *in situ* UV-VIS/Raman/XRD studied.

Keywords: *in situ* UV-VIS-DR spectroscopy, GC, heteropoly compound, reduction and oxidation, catalysis

1. Introduction

Due to their acidic and redox properties, heteropoly compounds (HPA) are considered to be promising catalysts for selective oxidation reactions, such as the conversion of isobutyric acid or methacrolein to methacrylic acid [1–5]. The broad compositional variability of HPA compounds allows the modification of their catalytic performance. For example, it was shown that the exchange of molybdenum for vanadium results in a higher redox potential in contrast to the vanadium-free compound. Recent work by Weismantel et al. [4] deals with the redox state of heteropoly acids, applying *ex situ* UV-VIS-NIR spectroscopy and *in situ* ESR. The first method has also been applied by other reseachers for the investigation of the electronic states of heteropoly compounds as catalysts [6–9]. It is thus known that the degree of reduction may be observed by spectral UV-VIS-NIR changes. Vanadium-containing compounds of the type $Cs_xH_{4-x}PVMo_{11}O_{40}{\cdot}nH_2O$ with $x = 0$–4 have characteristic absorption bands at about 660 and 1150 nm, which reflect the degree of reduction by the corresponding peak intensity and position. Beside these characteristic quantities, the absorption edge of the ligand to metal charge transfer band (LMCT) is also highly significant. LMCT transitions in many polyoxomolybdates are compiled and discussed by Fournier et al. [10]. Thus, a general red shift of the LMCT is observed with increasing degree of condensation of the polyoxometallates. When the heteropoly anions are heavily reduced, a heteropoly blue is produced and the intensity of the LMCT band should be reduced relative to the bands at lower energies [11,12].

Calculations of the band gap energy (E_g) were carried out by Weber [13] for polyoxomolybdates at room temperature. These investigations revealed that the E_g and the peak intensity of the band at about 660 nm of heteropoly compounds apparently change with increasing temperature in their reactive state due to structural alterations [14]. It is known for semiconductors that the E_g usually shifts to lower photon energy with increasing temperature. However, there is no information on the influence of the degree of reduction on the E_g of polyoxomolybdates [13].

The goals of this study were the investigation of the transient states during reduction/reoxidation and a correlation of the above mentioned spectroscopic quantities with catalytic data.

2. Experimental

2.1. Sample preparation

$H_4PVMo_{11}O_{40}{\cdot}nH_2O$, denoted HPA, was prepared from stoichiometric amounts of MoO_3, V_2O_5 and phosphoric acid in water [15]. The synthesis was followed by *in situ* UV-VIS spectroscopy. Cs_2CO_3 and the solution of heteropoly acid were used for the preparation of $Cs_2H_2PVMo_{11}O_{40}{\cdot}nH_2O$, denoted CsPA. Methanol and ethanol (Merck) were applied without further purification. He, purity >99.999 vol% and O_2, purity >99.998 vol% (Linde) were used without further purification.

* To whom correspondence should be addressed.

© J.C. Baltzer AG, Science Publishers

The catalyst samples had to be prepared such that the reflectivity was not too high for spectroscopy and, on the other hand, the conversion over these samples not too low for gas chromatographic detection of the gaseous products.

Mixtures of HPA or the salts of this heteropoly acid and quartz (Fluka) were made in the ratio of 1 : 13 by the incipient wetness method with an aqueous solution or suspension of the heteropoly compounds. The BET surface areas were 7 $m^2\,g^{-1}$ for the pure, calcined acid, 64 $m^2\,g^{-1}$ for CsPA and 1 $m^2\,g^{-1}$ for the support [15]. The reported measurements were carried out after outgassing in N_2/He at 200 or 250 °C for 1 h.

2.2. Techniques

2.2.1. UV-VIS spectroscopy

A Perkin–Elmer Lambda 9 spectrometer was used for *in situ* UV-VIS-DRS on different dilute catalyst samples. Approximately 600 mg were placed in a home-made microreactor cell operating under continuous gas flow. All spectroscopic measurements were sequentially carried out with a scan speed of 240 nm/min, a slit width of 5.0 nm and a response time of 0.5 s, with spectralon as a reference standard. All spectra were smoothed (smoothing intervall 20 nm) and the peak intensity of the IVCT band and the band gap energy (first derivation) were determined. The diffuse reflectance data were evaluated using the Kubelka–Munk (KM) equation.

The quantity δSP was defined as a structure parameter. It is calculated as follows:

$$\delta\mathrm{SP} = (E_{\mathrm{g,f}} - E_{\mathrm{g,i}}) \times 100/E_{\mathrm{g,i}}\ (\%),$$

with $E_{\mathrm{g,f}}$ the final apparent band gap energy at the end of the reduction/reoxidation and $E_{\mathrm{g,i}}$ the initial apparent band gap energy at room temperature (see section 3.2.1).

2.2.2. Gas chromatography

The gases were analyzed with a gas chromatograph (Perkin–Elmer), equipped with a heated automatic gas-sampling valve and a FFAP column (Machery–Nagel) using a flame ionization detector (FID). Due to this detection technique, oxidized species as CO and CO_2 cannot be quantified. A calculation of the carbon balance reveals a carbon misfit of ca. 10% for the methanol reactions, and of ca. 15% for the ethanol, respectively, pointing to carbon deposition on the catalyst.

The main products during the catalytic reaction of methanol and ethanol were dimethyl ether (DME), formaldehyde (FA), ethene (ET), diethyl ether (DEE) and acetaldehyde (ACA), respectively.

2.2.3. Catalytic test

The feed mixture was 25 ml/min helium, which was fed into saturators with methanol or ethanol, respectively, at 287 K (5 and 4 vol%, respectively) (SV 98000 $g^{-1}\,h^{-1}$), first co-fed with a stream of 50 ml/min helium then with 60 ml/min helium/oxygen (17 vol% oxygen in He). The total gas flow was kept constant at 75 ml/min for the reduction and 85 ml/min for the reoxidation. The catalysts were thermally pretreated in a flow of helium (100 ml/min) with a heating rate of 2.4 K/min up to 573 K prior to the reaction with the organic reactant. All catalytic reactions were conducted at 573 K. Blank experiments with quartz in the microreactor revealed methanol and ethanol conversions of about 1–2 and 8%, respectively.

3. Results

3.1. Conversion data

3.1.1. HPA and CsPA stoichiometric reduction

Figure 1(A) shows the conversion of methanol during the reaction over HPA and CsPA. An initial decrease in the conversion of methanol was not observed during the HPA reduction as detected over CsPA. From independent investigations of this compound, it is concluded that HPA is already thermally altered above 373 K [15]. Therefore, the initial catalytic activity and the deactivation process could not be detected in this experiment as for the ethanol reduction.

Over HPA the selectivity to DME over HPA initially increases slightly, while over CsPA it increases continuously with increasing time on stream, as shown in figure 1 (B) and (C). Over CsPA and HPA the selectivity to FA decreases correspondingly.

Figure 1(D) shows that the initial ethanol conversion over HPA and CsPA is much higher than that of methanol. A strong catalyst deactivation could be detected due to the lower reactivity of ethanol relative to methanol. The variation of the selectivities to ET, DEE and ACA with the time on stream is shown in figure 1 (E) and (F). The selectivity to ET initially decreases strongly for the CsPA catalyst (up to a reaction time of ca. 60 min) as compared to the selectivity decrease in the system ethanol/HPA. After 60 min reaction time, the selectivity to ET slightly decreases for the CsPA catalyst, while that over HPA remains nearly constant. The ACA selectivity over HPA remained almost constant, whereas the selectivity to ACA over CsPA increased more strongly until ca. 60 min time on stream. In contrast, the selectivity to DEE over both catalysts remained almost constant after an initial reaction time (figure 1 (E) and (F)).

3.1.2. HPA and CsPA reoxidation/catalysis

Figure 2(A) shows that the temporal change in the conversion of methanol during the reoxidation process of HPA strongly differs from that of CsPA. The initial conversion of methanol over HPA in presence of oxygen is lower than that during the reduction process and it increases with reoxidation time, only slowly approaching the final value of the reduction experiment. In the case of CsPA reoxidation in presence of methanol, the conversion is initially higher as compared to that of the reduction process and decreases with increasing reoxidation time. The selectivity to DME

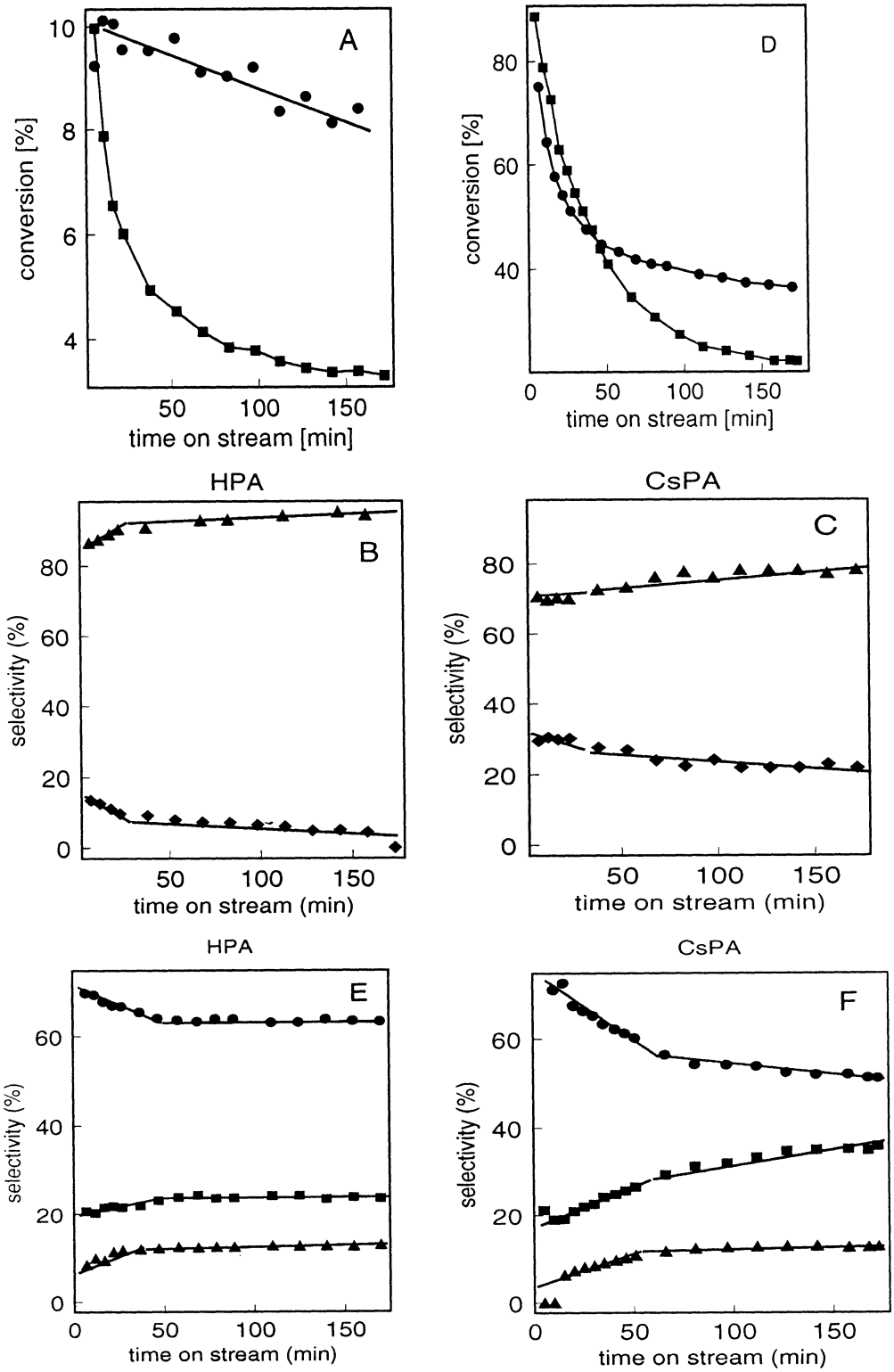

Figure 1. (A) Methanol conversion vs. time on stream upon reduction of $H_4PVMo_{11}O_{40}$ and $Cs_2H_2PVMo_{11}O_{40}$ at 573 K: (●) HPA, (■) CsPA. (B)–(C) Selectivity vs. time on stream upon reduction of $H_4PVMo_{11}O_{40}$ and $Cs_2H_2PVMo_{11}O_{40}$ by methanol at 573 K: (▲) DME over HPA and CsPA, (♦) FA over HPA and CsPA. (D) Ethanol conversion vs. time on stream upon reduction of $H_4PVMo_{11}O_{40}$ and $Cs_2H_2PVMo_{11}O_{40}$ at 573 K: (●) HPA, (■) CsPA. (E)–(F) Selectivity vs. time on stream upon reduction of $H_4PVMo_{11}O_{40}$ and $Cs_2H_2PVMo_{11}O_{40}$ by ethanol at 573 K: (●) ET over HPA and CsPA, (■) ACA over HPA and CsPA, (▲) DEE over HPA and CsPA.

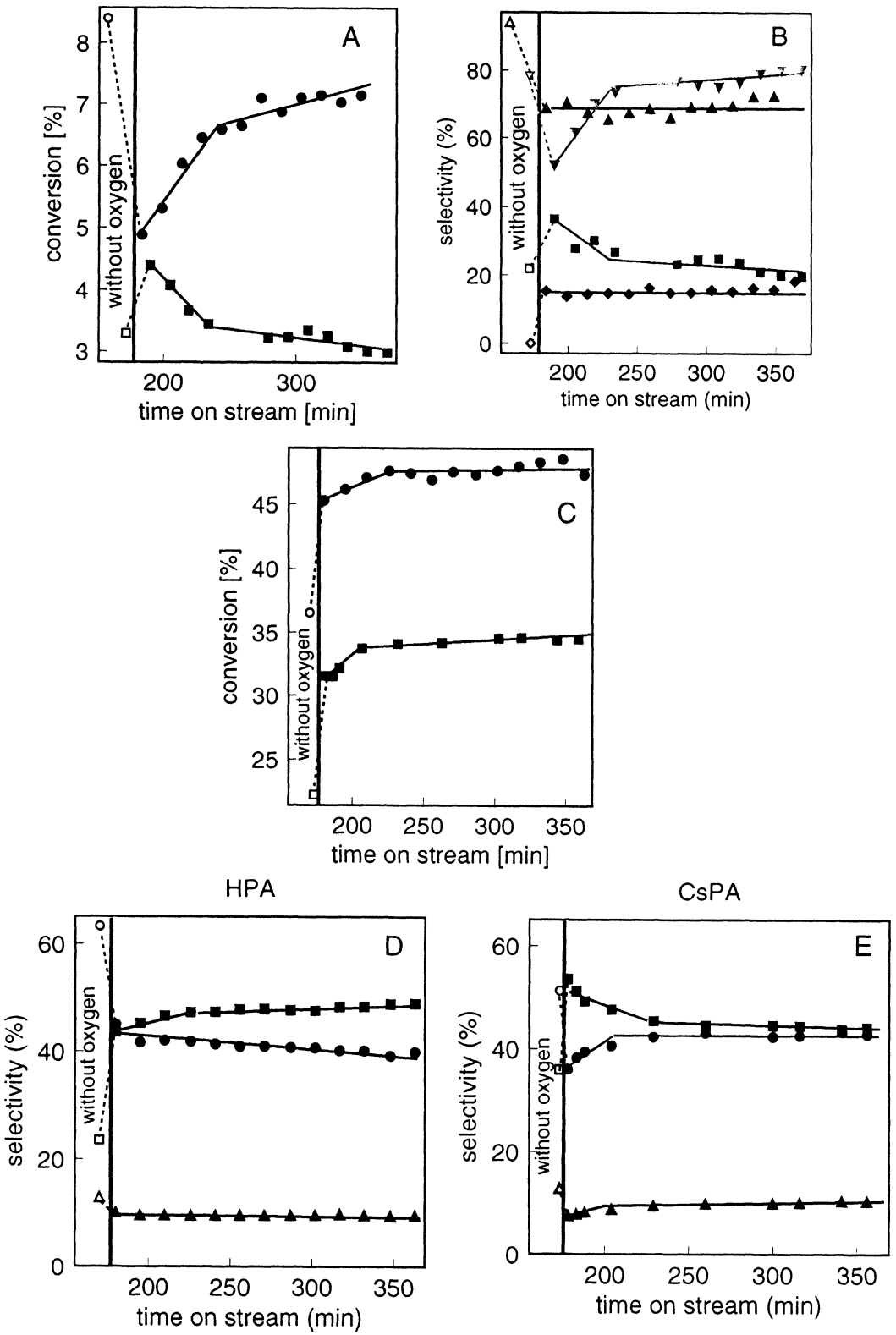

Figure 2. (A) Methanol conversion vs. time on stream upon reoxidation of $H_4PVMo_{11}O_{40}$ and $Cs_2H_2PVMo_{11}O_{40}$ at 573 K: (●) HPA, (■) CsPA. (B) Selectivity vs. time on stream upon reoxidation of $H_4PVMo_{11}O_{40}$ and $Cs_2H_2PVMo_{11}O_{40}$ by methanol at 573 K: (△ , ▲) DME over HPA, (◇ , ♦) FA over HPA, (▽ , ▼) DME over CsPA, (□ , ■) FA over CsPA. (C) Ethanol conversion vs. time on stream upon reoxidation of $H_4PVMo_{11}O_{40}$ and $Cs_2H_2PVMo_{11}O_{40}$ at 573 K: (●) HPA, (■) CsPA. (D)–(E) Selectivity vs. time on stream upon reoxidation of $H_4PVMo_{11}O_{40}$ and $Cs_2H_2PVMo_{11}O_{40}$ by ethanol at 573 K: (○ , ●) ET over HPA and CsPA, (△ , ▲) DEE over HPA and CsPA, (□ , ■) FA over HPA and CsPA.

and FA over HPA nearly remains constant. It is smaller in the case of DME/HPA than the value obtained during reduction, as shown in figure 2(B). Figure 2(B) also shows that the selectivity to FA over CsPA decreases, and that to DME increases with time on stream.

During the reoxidation of both ethanol-reduced catalysts, an increase of the conversion is observed relative to the conversion levels reached after the reduction step. Figure 2(C) shows this successive increase in conversion during the first 30 min of reoxidation. The conversion reaches steady state for longer times on stream.

In the selectivity/time on stream plots shown in figure 2 (D) and (E), a complex relation is revealed between the formation of the acid-catalyzed product ET and the selective oxidation product ACA. The selectivity to the coupling product DEE – 10% – is comparable over both catalysts and independent of the conversion level. The selectivity to ET over HPA decreases and that to ACA over HPA (selective oxidation) increases with increasing time on stream (figure 2(D)). Initially, the exact opposite behaviour is found for the CsPA catalyst with the same magnitude of the changes for both catalysts, but subsequently the selectivity to ET and ACA becomes independent of time on stream (figure 2(E)).

Acid properties play a role in the reaction of ethanol over heteropoly compounds, as evidenced by the formation of ET. Similar to investigations of the reduction of heteropoly compounds by methacrylic acid, in which propene was detected as a product [4,16], an initial linear decrease in the catalytic activity to ET was observed, which is more pronounced in the case of CsPA than HPA. In order to compare the catalytic data with those in the literature [17], the different selectivities were used as selectivity ratios of ethers to aldehydes. This ratio is a measure of the acidic versus the redox catalytic properties. The steady-state selectivity ratio of DME and FA (during the methanol reaction) – ca. 7 and 4 during the oxidation process of methanol/HPA and methanol/CsPA, respectively – is significantly larger than those reported in the literature [18,19]. This observation seems to point to poorer redox catalytic properties of the catalyst under study, perhaps due to excessive reduction pretreatment.

3.2. In situ UV-VIS spectroscopic characterization of the heteropoly compounds

3.2.1. Thermal treatment of heteropoly compounds

Heteropoly compounds lose crystal and constitutional water upon heating. In figure 3, the loss of water is reflected by an increase of the absorption in the low-frequency region of the visible spectrum. In addition, an absorption band develops at about 660 nm with growing intensity when HPA is heated above 371 K, and at 690 nm when CsPA is heated above 438 K. A very broad absorption band between 350 and 420 nm (CsPA and HPA) is also observed. The peak intensity of this band seems to decrease with increasing temperature. The intensity of the absorption due to the valence

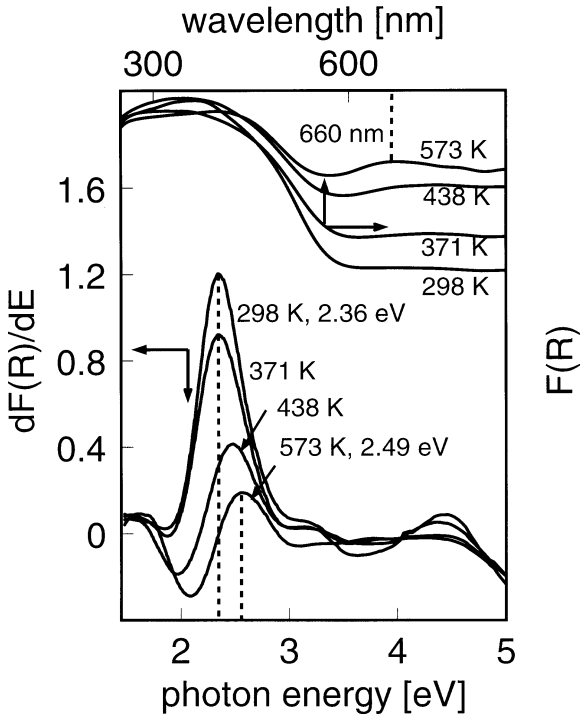

Figure 3. *In situ* UV-VIS diffuse reflectance spectra of $H_4PVMo_{11}O_{40}$ (above) and first derivates versus photon energy (below) during the thermal treatment under helium: (1) 2.36 ± 0.02 eV at 298 K; (2) 2.36 ± 0.02 eV at 371 K; (3) 2.47 ± 0.02 eV at 438 K; (4) 2.49 ± 0.02 eV at 573 K.

to conduction band transition becomes weaker with increasing temperature relative to the Mo^{5+} d–d transitions/intervalence transfer band intensity (*vide infra*).

The band edge of CsPA does not exhibit a sharp edge feature which is characteristic of oxide semiconductors. A weak absorption band is superimposed on the edge, as seen most clearly in the spectrum recorded at room temperature (not shown).

The E_g determined for HPA increases from 2.36 ± 0.02 eV (298 K) to 2.49 ± 0.04 eV (573 K) (figure 3) and the apparent band gap energy E_g^* of CsPA increases from 2.45 ± 0.02 eV (298 K) to 2.59 ± 0.003 eV (573 K) (not shown). According to Fournier et al. [10], the increase of the E_g^* can be attributed to a structural alteration of the polyacid catalysts. The E_g^*s determined at room temperature are comparable to those of other compounds, e.g., 2.72 eV for $(\text{tetrabutylammonium})_2Mo_6O_{19}$ and 3.31 eV for $(NH_4)_6Mo_7O_{24}$ [13]. No data are found in the literature for the E_g^* values at high temperatures.

The broad bands between 350 and 420 nm are assigned to a strong LMCT which are also known as the second-lowest energy charge transfer bands [20]. The band at about 660–685 nm is attributed to an IVCT band [21–23]. It may be assigned to a charge transfer from V^{4+} to Mo^{6+}, however, d–d transition of Mo^{5+} ($^2B_2 \rightarrow {}^2E$) cannot be excluded [6,24].

3.2.2. Stoichiometric reduction

Figure 4 shows a strongly increasing absorption in the low-frequency region of the visible spectrum immediately

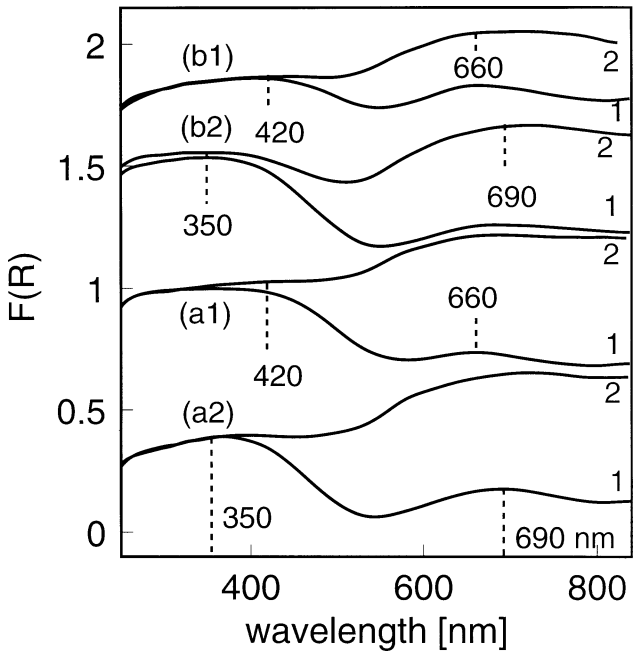

Figure 4. *In situ* UV-VIS diffuse reflectance spectra of $H_4PVMo_{11}O_{40}$ and $Cs_2H_2PVMo_{11}O_{40}$ during the methanol and ethanol reaction without and with oxygen at 573 K. Methanol reaction: (a1) HPA and (a2) CsPA; ethanol reaction: (b1) HPA and (b2) CsPA; (a1), (a2), (b1) and (b2) time on stream (min): 3 (1) and 172 (2). For a better visualization the ethanol spectra were vertically shifted.

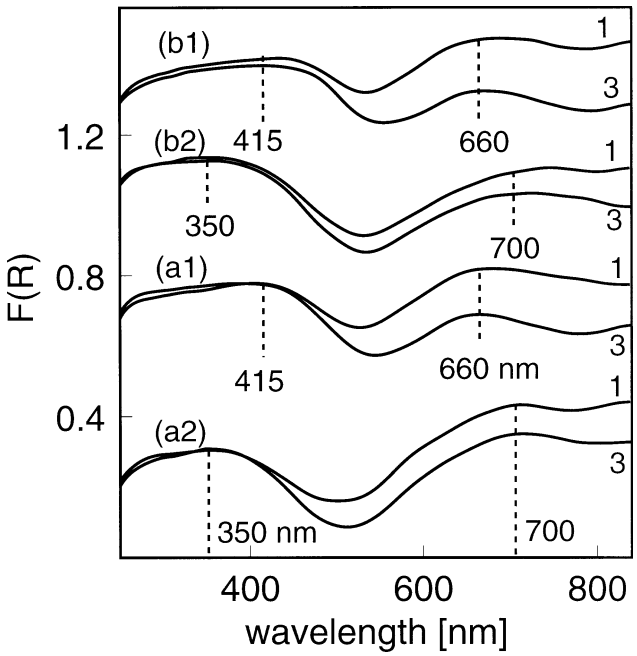

Figure 5. *In situ* UV-VIS diffuse reflectance spectra of $H_4PVMo_{11}O_{40}$ and $Cs_2H_2PVMo_{11}O_{40}$ during the methanol and ethanol reaction without and with oxygen at 573 K. Methanol reaction: (a1) HPA and (a2) CsPA; ethanol reaction: (b1) HPA and (b2) CsPA; (a1), (a2), (b1) and (b2) time on stream (min): 3 (1) and 172 (2). For a better visualization the ethanol spectra were vertically shifted.

after introducing methanol or ethanol in the gas feed. This feature indicates the partial reduction of the HPA giving rise to a variety of absorption bands [25]. The increase is more pronounced in the presence of methanol than ethanol, indicating the higher reactivity of methanol. A much stronger increase in absorption in the low-frequency region of the visible spectrum of CsPA is initially also observed for methanol than for ethanol, indicating the higher reactivity of methanol than ethanol. During reduction by methanol, there is only a scarcely perceptible change in the spectra after a reaction time of ca. 30 min (not shown). An initially increasing broadening of the IVCT peak is detected during reduction of the heteropoly compounds with time on stream. A broad peak at about 660 nm is observed during the thermal pretreatment of HPA (figure 3). This peak is weaker in presence of ethanol than methanol, again indicating the lower reactivity of ethanol than methanol. The peak maximum of the broad absorption band at 350 nm of the CsPA has shifted by 70 nm to lower wavelengths as compared to the results on the HPA. The initial increase in the spectral absorption at 690 nm during the reduction process of CsPA is evident in figure 5.

3.2.3. Catalytic operation

Figure 5 shows the UV-VIS-DR spectra during reoxidation of both catalysts. The absorption decreases with increasing reoxidation time, but the difference between the absorption levels observed initially and at the end of reoxidation is significantly smaller than in the case of reduction (figures 4 and 5). As expected, reoxidation reverses the reduction phenomena without, however, forming the initial spectral properties of both catalysts.

3.2.4. Temporal change of the IVCT band and the apparent band gap energy

Figure 6 shows that the value of E_g^* and the peak intensity of the IVCT band initially increase during HPA reduction. After a reaction time of ca. 30 min both spectroscopic quantities are independent of the time on stream. The initial increase in the peak intensity of the IVCT band and of the E_g^* of HPA, which is more pronounced for methanol than for ethanol reduction, is evident from the data in figure 6. In contrast, the peak intensity of the IVCT band of HPA under methanol is weaker than that under ethanol.

The stronger fluctuation of the peak intensity data of CsPA is striking as compared to that of the HPA, which is stronger than that of the E_g^* (not shown). However, the response of the spectroscopic quantities is comparable to that of the HPA.

In addition, these quantities already remain constant after ca. 10 min reoxidation while both spectroscopic quantities become constant after 30 min time on stream during reduction. The introduction of oxygen in the gas feed leads to fast decrease of the IVCT absorption. Again, E_g^* is larger and the peak intensity of the IVCT band is weaker for methanol over CsPA in comparison to ethanol for reduction and reoxidation. A small increase in E_g^* is observed in the ethanol/CsPA system.

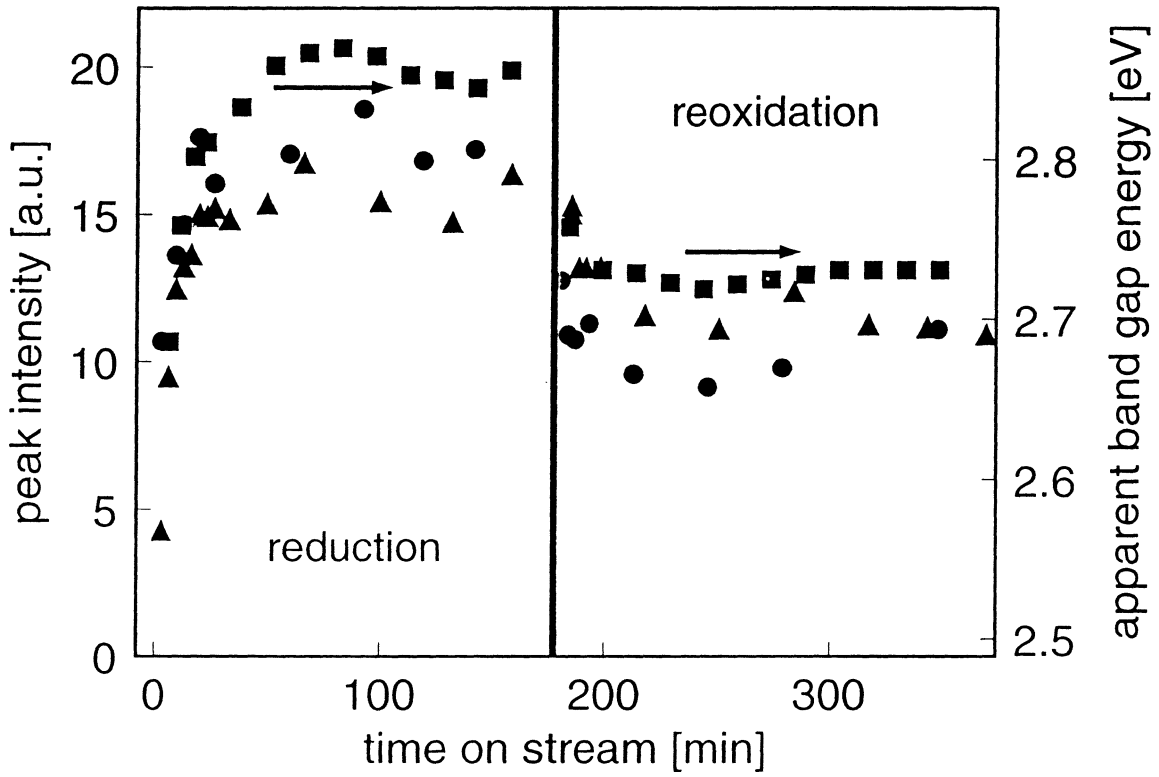

Figure 6. Spectroscopic data for reduction of $H_4PVMo_{11}O_{40}$ by methanol and ethanol and subsequent reoxidation at 573 K: (▲) peak intensity, (■) E_g^* of methanol over HPA; (●) peak intensity, (♦) E_g^* of ethanol over HPA.

3.3. Correlation between catalytic and spectroscopic data

A correlation between catalytic and spectroscopic data would highlight the relevance of the spectroscopic data for the characterization of the active catalyst under steady state. The steady-state data obtained for the reduced and reoxidized states of the two catalysts were used to define two levels of catalytic performance under comparable conditions. The usual procedure of varying the gas phase or flow conditions to test for the catalytic performance was not applied, as it is not known in which way the structure of the catalyst depends on these variables.

Figure 7 summarizes the obtained data. It is evident that the data obtained for methanol do not show the expected trend. This unexpected behaviour can only be explained by too deep a reduction/alteration of the catalysts in presence of the reactive methanol as compared to ethanol. In this case, it is impossible to regenerate the state of the active catalyst by oxygen addition in the feed. For the reaction with the less reactive ethanol, the situation is different, as seen from the expected correlation of higher conversions with lower degrees of reduction. The two catalysts exhibit the same trend at different levels.

This restricted data set allows only the conclusion that the electronic structure/degree of reduction as measured by the structure parameter δSP is relevant for the catalytic performance. Future experiments are necessary to characterize the real structure of the active catalyst and to correlate this

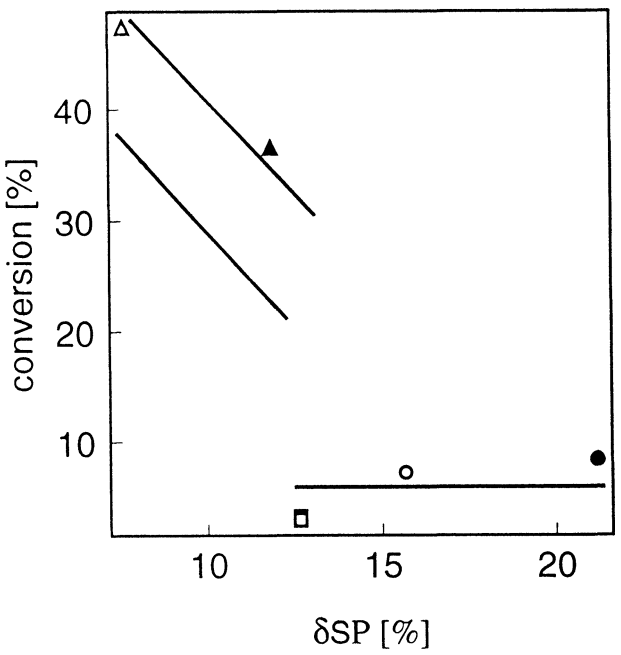

Figure 7. Conversion vs. δSP for reduction and reoxidation of $H_4PVMo_{11}O_{40}$ and $Cs_2H_2PVMo_{11}O_{40}$ by methanol and ethanol without and with oxygen at 573 K: (●) reduction, (○) reoxidation: methanol over HPA; (▲) reduction, (△) reoxidation: ethanol over HPA; (■) reduction, (□) reoxidation: methanol over CsPA; (▼) reduction, (▽) reoxidation: ethanol over CsPA.

structure with the degree of reduction and the catalytic performance.

4. Discussion

A partially reduced state of the heteropoly compounds, which is already produced by thermal pretreatment, is characterized by an increased absorption in the low-frequency region of the visible spectra, brought about by the change of the IVCT band. The shift of the E_g^* to higher values and the gradual increase of the peak intensity of the IVCT band with reduction time indicates that the geometric and electronic structure of the catalyst material changes upon heating to 573 K in inert gas (figure 3).

The electronic structure of the catalysts during the alcohol reduction (time on stream $>$30 min), as compared to the room temperature Keggin structure, reveals a more pronounced alteration than that under inert gas atmosphere at 573 K. Unfortunately, no final conclusions about the catalyst structure can be drawn from the changes in the position and intensity of the LMCT band during alcohol reactions.

The flattening of the edge feature and the increase of the absorption above 600 nm with a broadening of the IVCT band (figure 4) indicates that the catalyst is in the reduced state during catalysis. The shift of the LMCT transition may point to geometric alterations of the Keggin anions.

The fact that Cs incorporation reduces the catalytic activity is consistent with this view, as the spatial requirements for the structural reorganization within each unit cell of the solid are not fulfilled in the presence of the space-filling Cs ion. Their positive effect on catalyst lifetime, on the other hand, may be attributed to the inhibition of the polymerization into extended MoO_3.

Upon the change in the gas phase from reduction to catalytic conversion, a partial reoxidation occurs (decrease of the absorption, figure 5) without restoring the initial fully oxidized state. This points to the importance of both reactants for the stabilization of a slightly reduced state of the catalyst, which has defect electrons energetically located in the band gap. The data of the spectroscopic and catalytic properties also correlate in this time-dependent operation as may be concluded from a comparison of the figures 2 and 6.

From the increase in the selectivity ratio of DME and FA and the successive increase in the intensity of the IVCT band and that of the E_g^* (figure 6), it can be concluded that the degree of reduction of HPA and CsPA during the reduction process also influences the formation of DME (see section 3.1.1). In the methanol/heteropoly systems, only a smaller portion of oxygen vacancies is reoxidized than in the case of the ethanol/heteropoly compounds, which indicates a higher reactivity of methanol. Too deep a reduction of the catalyst obviously has a negative effect on the alcohol conversion.

Catalytic and spectroscopic data measured during reduction of the heteropoly compounds by alcohols can be correlated. This becomes particularly evident at the beginning of the reduction process when a decrease/increase in the conversion/selectivity ratio results in a parallel increase of the peak intensity of the IVCT band and with an increase of E_g^*. The selectivity ratios reveal that the selective oxidation activity decreases with an increasing degree of reduction.

The reason for the low methanol conversion compared to that of ethanol can be related to a deeper reduction of the catalyst after reduction by methanol ($E_0 = 0.04$ V) than by ethanol ($E_0 = 0.17$ V). This fact is reflected in figure 7, which shows that a larger δSP after reduction by methanol results in lower conversions over both heteropoly compounds to ethanol.

The trend that higher absolute values of the spectroscopic parameters, which indicate a higher degree of reduction, are counter-productive for the level of conversion is observed in the data of figure 7. During reoxidation in presence of methanol the partial pressure of oxygen is less effective in reoxidizing the catalyst than during reoxidation in presence of ethanol. Consequently, no temporal change can be seen in spectroscopy and catalysis. Thus, the correlation between changes of conversion and δSP can be seen clearly for the ethanol systems but not for the methanol reactions.

5. Conclusion

The evolution of the absorption band edge of the initially well-defined HPA semiconductors into a complex structure is seen as indication that the Keggin molecular units break down upon thermal (initial deactivation after pretreatment) and catalytic load. It develops into a solid with a different electronic structure which cannot be fully characterized with the present *in situ* UV-VIS-DRS method alone. It is suggested that the spectra shown here can be taken as indication of a structural reorganization of the initial molecular Keggin units with a reduced vanadium–oxygen group. The data presented show clearly that the room temperature Keggin structure is not preserved in the catalytically active form of the catalysts. The Keggin anions act, therefore, only as catalyst precursors. The actual molecular structure of this catalytically active species, however, remains unknown. UV-VIS-DR spectra do not show enough resolution for a structural analysis, and future *in situ* Raman, IR and XRD experimets are required. The degree of reduction, however, is critical to catalytic performance as the data prove that over-reduction is counter-productive for the alcohol conversion.

Under stoichiometric reaction conditions, it is evident from the UV-VIS-DR spectra that lattice oxygen contributed to the activity. The oxygen defects, however, could not fully be replenished by reoxidation. The experimental data cannot yet be considered as a proof of the Mars–van Krevelen mechanism, since no evidence of a direct involvement of lattice oxygen under catalytic conditions can be derived from the transient or dynamic behaviour of the

system. This evidence is currently being sought in time-resolved *in situ* experiments probing conversion, electronic structure and geometric structure simultaneously.

Acknowledgement

The authors are indebted to S. Berndt for preparing the heteropoly compounds and to M. Thiede for the experimental assistance in UV-VIS spectroscopy.

References

[1] C. Desquilles, M.J. Bartoli, E. Bordes, G. Hecquet and P. Courtine, Petrochemie 109 (1993) 130.
[2] A. Aboukakaïs, D. Ghoussoub, E. Blouet-Crusson, M. Rigole and M. Guelton, Appl. Catal. 111 (1994) 109.
[3] Th. Ilkenhans, B. Herzog, Th. Braun and R. Schlögl, J. Catal. 153 (1995) 275.
[4] L. Weismantel, J. Stöckel and G. Emig, Appl. Catal. 137 (1996) 129.
[5] L.M. Deußer, J.W. Gaube, F.-G. Martin and H. Hibst, Stud. Surf. Sci. Catal. B 101 (1996) 981.
[6] G. Centi, J. Lopez Nieto and C. Iapalucci, Appl. Catal. 46 (1989) 197.
[7] G. Centi, V. Lena, F. Trifirò, D. Ghoussoub, C.F. Aissi, M. Guelton and J.P. Bonnelle, J. Chem. Soc. Faraday Trans. 86 (1990) 2775.
[8] D. Casarini, G. Centi, P. Jiru, V. Lena and Z. Tvarùzková, J. Catal. 143 (1993) 325.
[9] N.N. Timofeeva, A.V. Demidov, A.A. Davydov and I.V. Kozhevnikov, J. Mol. Catal. 79 (1993) 21.
[10] M. Fournier, C. Louis, M. Che, P. Chaquin and D. Masure, J. Catal. 119 (1989) 400.
[11] E. Papaconstantinou and M.T. Pope, Inorg. Chem. 9 (1970) 667.
[12] M. Pope, *Heteropoly and Isopoly Oxometalates in Inorganic Chemistry Concepts* (Springer, Berlin, 1983).
[13] R.S. Weber, J. Catal. 151 (1995) 470.
[14] J. Melsheimer, G. Schulz, M. Thiede, G. Mestl and R. Schlögl, to be published.
[15] S. Berndt, D. Herein, F. Zemlin, E. Beckmann, G. Weinberg, J. Schütze, G. Mestl and R. Schlögl, Ber. Bunsen Ges. Phys. Chem. 102 (1998) 763.
[16] T. Haeberle and G. Emig, Chem. Eng. Technol. 11 (1988) 392.
[17] K. Brückman, M. Che, J. Haber and J.-M. Tatibouët, Catal. Lett. 25 (1994) 225.
[18] K. Brückman, J. Haber and E.M. Serwicka, Faraday Discuss. Chem. Soc. 87 (1989) 173.
[19] K. Brückman, J.-M. Tatibouët, M. Che, E. Serwicka and J. Haber, J. Catal. 139 (1993) 455.
[20] K. Nomiya, Y. Sugie, K. Amimoto and M. Miwa, Polyhedron 6 (1987) 519.
[21] H. So and M.T. Pope, Inorg. Chem. 11 (1972) 1441.
[22] J.J. Altenau, M.T. Pope, R.A. Prados and H. So, Inorg. Chem. 14 (1975) 417.
[23] R. Buckley and R.J.H. Clark, Coord. Chem. Rev. 65 (1985) 167.
[24] C. Sanchez, J. Livage, J.P. Launay, M. Fournier and Y. Jeannin, J. Am. Chem. Soc. 104 (1982) 3194.
[25] P. Gómez-Romero and N. Casañ-Pastor, J. Phys. Chem. 100 (1996) 12448.